International Journal Of Engineering Research And Development
e- ISSN: 2278-067X, p-ISSN: 2278-800X, www.ijerd.com
Volume 20, Issue 3 (March. 2024), PP. 265-278

Simulation of Focused Thermal Ablation of Brain Tumors using a Precise Microwave Antenna Approach in COMSOL Multiphysics

Bubu Pius Erheyovwe, PhD
[1]*Department of Biomedical Engineering, School of Engineering and Applied Sciences*
Kampala International University, Western Campus, Bushenyi-Ishaka, Uganda
Corresponding Author: bubupius.e@kiu.ac.ug.

ABSTRACT
Microwave ablation has emerged as a promising alternative, offering a minimally invasive and highly targeted approach to brain tumor eradication following Filippiadis et al. (2016). This study utilized COMSOL Multiphysics 6.2 simulation to assess the impact of microwave ablation on brain tumors operating at a frequency of 1.45 GHz. Key findings include focused power dissipation density and temperature rise within the targeted area, indicating the effectiveness of the ablation process. The simulation results, supported by existing literature, highlight the precise targeting capabilities of the microwave antenna with minimal thermal spread to surrounding healthy tissue.
The analysis highlights microwave ablation as a highly effective treatment for brain tumors, aiming for precise tumor elimination while protecting surrounding structures. Comparing with existing literature like strengthens the evidence for microwave ablation as a promising strategy. Simulation data offers insights for optimizing treatment and improving outcomes, emphasizing the importance of microwave ablation in fighting brain tumors. Overall, microwave ablation technology represents a significant advancement in neuro-oncology, offering hope for patients with limited treatment options. By using electromagnetic radiation, microwave ablation has the potential to transform brain tumor management, leading to better patient outcomes and survival rates.

Date of Submission: 15-03-2024 Date of Acceptance: 31-03-2024

I. INTRODUCTION)

Brain tumors pose a significant challenge in the field of oncology, as they present a wide range of clinical, therapeutic, and scientific obstacles (Ostrom, 2019). The incidence rate of brain tumors is increasing worldwide, and they encompass a diverse range of neoplastic entities, varying from benign to malignant and primary to metastatic. Despite advancements in diagnostic imaging, surgical procedures, and additional treatments, effectively managing brain tumors remains a difficult task, resulting in less suboptimal outcomes.

1.1 **Background Information on Brain Tumors and Current Treatment Methods**

Brain tumors are a diverse group of malignancies characterized by abnormal cell growth within the brain or its surrounding structures. They can be primary, originating from cells within the brain, or metastatic, spreading to the brain from cancers elsewhere in the body (Li & Graeber, 2012). The clinical presentation of brain tumors varies depending on factors such as tumor size, location, histology, and growth rate. Symptoms may include headaches, seizures, neurological deficits, cognitive impairment, and changes in behavior.

Current treatment strategies for brain tumors involve a multidisciplinary approach tailored to the specific characteristics of the tumor and the patient. Surgical resection is often the mainstay of therapy for accessible tumors, aiming to remove as much of the tumor as possible while preserving neurological function (Farag et al., 2019; Matar et al., 2018). However, some tumors are challenging to completely remove due to their complex anatomy and infiltrative nature, requiring additional treatments like radiotherapy and chemotherapy to address any remaining disease (Stupp et al., 2005).

Radiation therapy, delivered either through external beam radiotherapy or stereotactic radiosurgery, plays a crucial role in managing both primary and metastatic brain tumors. It effectively targets tumor cells while minimizing damage to healthy surrounding tissue (Barker et al., 2015). Chemotherapy, either alone or in combination with radiation therapy, is used to treat certain high-grade gliomas and metastatic brain tumors by targeting rapidly dividing tumor cells through various mechanisms (Stupp et al., 2005).

Despite the availability of these treatment options, the prognosis for many brain tumor patients remains poor (Chinot, 2012). Recurrence rates are high, treatment-related side effects can be significant, and there are

limited therapeutic options for cases that do not respond to standard treatments (Stupp et al., 2005). Moreover, the inherent heterogeneity of brain tumors poses a significant challenge to the development of targeted therapies, highlighting the need for innovative approaches that can effectively target tumor cells while sparing normal brain tissue.

1.2 **The Need for New Treatment Modalities**

The critical need for the development of new therapeutic strategies that can overcome the challenges posed by current treatment methods and improve outcomes for patients with brain tumors is emphasized by the limitations of these modalities (Cancer Research UK, 2024; Ostrom et al., 2018). Traditional approaches like surgery, chemotherapy, and radiotherapy often result in significant morbidity and mortality, especially in cases of high-grade or recurrent disease (Stupp et al., 2009; Louis et al., 2016). Surgical resection, although effective in many cases, is restricted by the infiltrative nature of certain tumors and the potential risk of damaging critical neurovascular structures (Siker et al., 2011). Chemotherapy, while capable of targeting rapidly dividing tumor cells, is frequently hindered by systemic toxicity and the emergence of drug resistance (Lassen et al., 2013). Similarly, radiotherapy, while providing localized tumor control, can cause long-term neurocognitive deficits and radiation-induced toxicity in the surrounding brain tissue (Greene-Schloesser et al., 2013).

Moreover, the inherent heterogeneity of brain tumors poses a significant challenge to the development of targeted therapies (Patel et al., 2014). The molecular and genetic makeup of individual tumors can vary greatly within and between patients, making it difficult to devise effective treatments (Verhaak et al., 2010). Precision medicine approaches, which aim to customize treatment strategies based on the unique molecular profile of each patient's tumor, offer promise for improving therapeutic outcomes (Chin et al., 2011). However, the implementation of precision medicine in clinical practice is impeded by various logistical, technical, and regulatory obstacles (Roychowdhury et al., 2011). This underscores the need for alternative approaches that can effectively target tumor cells while minimizing harm to healthy tissue.

1.3 **An Overview of Microwave Ablation Technology**

Microwave ablation has emerged as a promising therapeutic method for treating brain tumors. It offers a minimally invasive approach that specifically targets and destroys tumor tissue, without affecting healthy structures. Unlike traditional treatments like surgery, chemotherapy, or radiotherapy, microwave ablation utilizes electromagnetic radiation to selectively heat and eliminate tumor cells.

The principle behind microwave ablation involves the interaction between electromagnetic waves and biological tissues. By converting microwave energy into heat through dielectric heating mechanisms, the water molecules within the tumor tissue rapidly absorb the energy. This leads to localized heating, causing necrosis and cell death within the tumor while preserving the surrounding normal tissue.

One of the main advantages of microwave ablation is its ability to rapidly and uniformly generate high temperatures within the tumor tissue. This results in more efficient tumor eradication compared to other thermal ablation methods like radiofrequency ablation or cryoablation. Additionally, microwave ablation can be performed using minimally invasive techniques, reducing the risk of surgical complications and enabling treatment of tumors in deep or inaccessible areas of the brain (Lubner et al., 2010).

Furthermore, microwave ablation allows for real-time monitoring during the procedure. Advanced imaging modalities such as magnetic resonance imaging (MRI) or computed tomography (CT) can be used to precisely locate and target the tumor tissue (Trigg et al., 2020). This ensures accurate placement of the ablation probe and complete coverage of the tumor, while minimizing damage to critical adjacent structures (Filippiadis et al., 2018).

II. MATERIAL AND METHODS

The study utilized the RF Module of COMSOL Multiphysics to simulate the electromagnetic waves in the frequency domain. The geometric entity level was set to the domain, encompassing all domains within the geometry. The electric field components were solved for as a three-component vector, and the mesh was controlled by physics with a maximum element size parameter derived from the study. The methodology was set to ‘Fast’ to optimize the simulation process.

The materials used, Figure 2.1 in the COMSOL analysis for the simulation of microwave ablation in brain tissue are described as follows:

Brain (Human):

i. **Relative Permittivity (ε):** Denoted as eps_brain, this parameter represents how much the brain tissue can polarize in response to an electric field, affecting how the electromagnetic waves propagate through it.
ii. **Relative Permeability (μ):** With a value of 1, it indicates that the brain tissue does not magnetize in response to a magnetic field.

iii. **Electrical Conductivity (σ):** Represented as sigma_brain, it measures the brain tissue's ability to conduct electricity, which is crucial for determining how it heats up when exposed to microwaves.
iv. **Density (ρ):** At 1000 kg/m³, it is used to calculate mass-related properties like the specific heat capacity.
v. **Thermal Conductivity (k):** The k is the brain's thermal conductivity where the value of 0.52 W/(m·K) used indicates how well the brain tissue can conduct heat.
vi. **Activation Energy (Δ*E*):** With a value of 2.577E5 J/mol, it is part of the Arrhenius equation parameters that describe the rate of the chemical reactions occurring during heating.
vii. **Frequency Factor (A):** A high value of 7.39E39 1/s suggests a significant reaction rate, also part of the Arrhenius equation.
viii. **Heat Capacity at Constant Pressure (Cp):** At 3540 J/(kg·K), it determines how much energy is required to raise the temperature of the brain tissue.

Catheter:

i. **Relative Permittivity (ε):** Denoted as eps_cat, it is likely close to 1, indicating that the catheter material has minimal impact on the electric field.
ii. **Electrical Conductivity (σ):** A value of 0 S/m means the catheter is an insulator and does not conduct electricity.
iii. **Dielectric:**
iv. **Relative Permittivity (ε):** Labeled as eps_diel, similar to the catheter, it likely has a minimal impact on the electric field.

Air:

Relative Permittivity (ε) and Relative Permeability (μ): Both have values of 1, indicating standard conditions for air, which does not significantly affect the electric or magnetic fields.

Functions:

These are likely used to define temperature-dependent properties such as thermal conductivity (k), specific heat capacity (Cp), and density (ρ), which are essential for accurately simulating the thermal response of the materials to microwave heating. The material properties and functions defined in the COMSOL model are critical for accurately simulating the interaction of microwaves with brain tissue and the catheter, according to Table 2. They ensure that the physical behavior of the materials under the influence of electromagnetic fields and heat is correctly represented, which is essential for predicting the outcome of the microwave ablation procedure. The overall implication for the title of the study is that these material parameters allow for a precise and realistic simulation of the thermal ablation process, supporting the research's focus on targeted cancer treatment using microwave technology.

Microwave Antenna Design for Brain Tumor Ablation

The antenna system described herein is engineered for the precise delivery of microwave energy to brain tumors for thermal ablation therapy. As depicted in Figure 2.1, the antenna's geometry is defined by a thin coaxial cable, which features a ring-shaped slot with a 1 mm width, strategically positioned 5 mm from the antenna's short-circuited tip. This configuration is crucial for the controlled emission of microwaves into the targeted brain tissue.

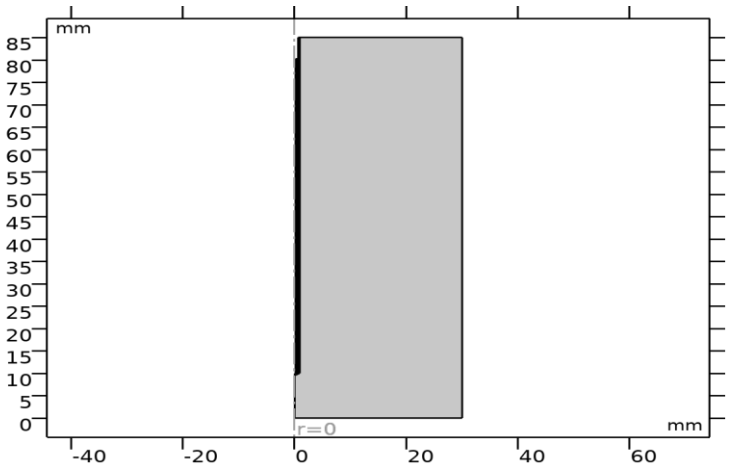

Figure 2.1: The antenna's geometry

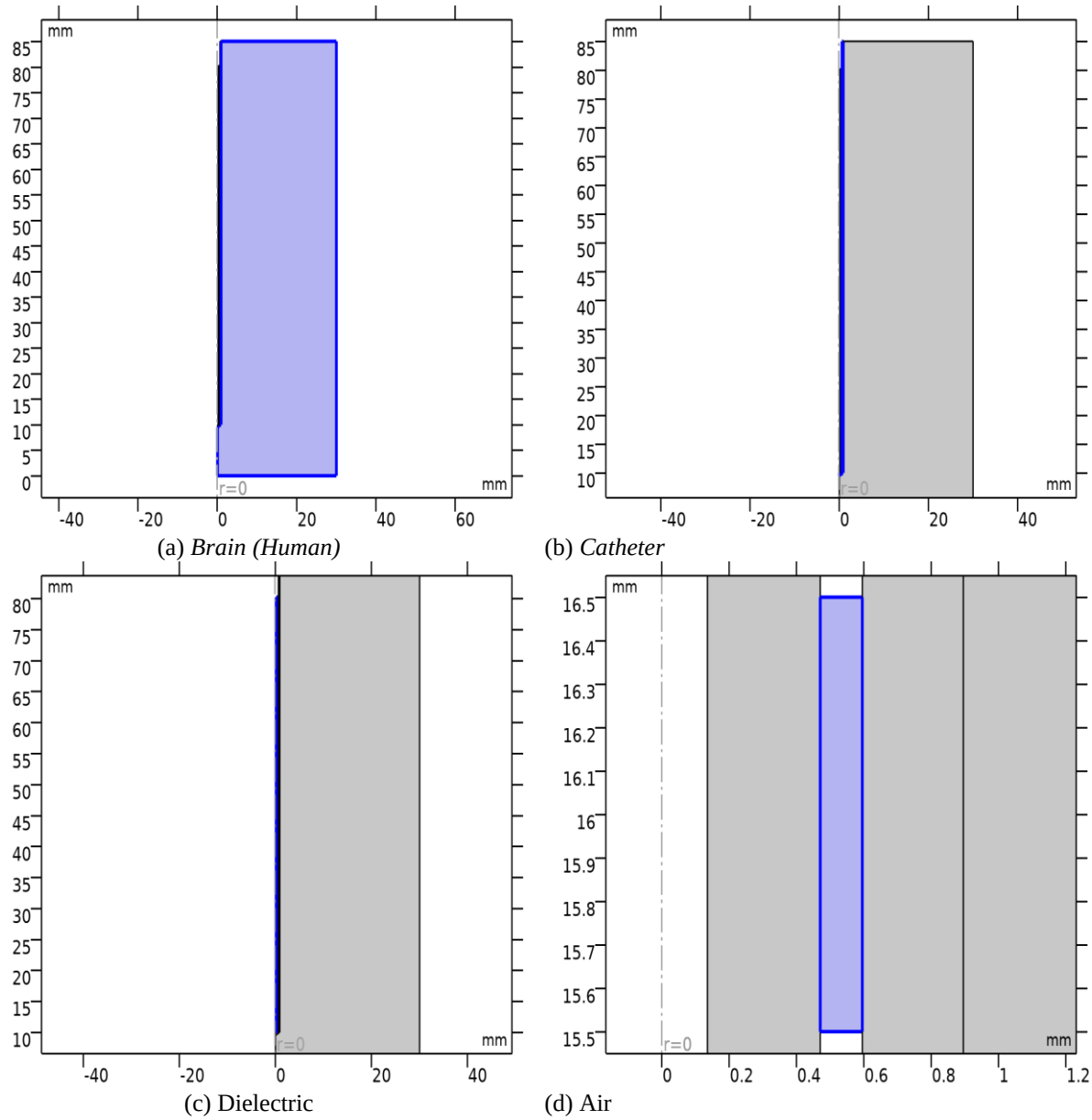

(a) *Brain (Human)* (b) *Catheter*

(c) Dielectric (d) Air

Figure 2.2: Materials Used

To maintain sterility and ensure biocompatibility, the entire antenna assembly is encased within a catheter composed of PTFE (polytetrafluoroethylene), a material known for its non-reactive properties. The geometrical dimensions and material data are detailed in the accompanying tables, providing a comprehensive overview of the antenna's structure. Operating at a frequency of 1.45 GHz, which is commonly utilized in microwave coagulation therapy, the antenna is optimized for the ablation of cancerous cells without affecting the surrounding healthy tissue. The design leverages the problem's inherent rotational symmetry, allowing for a two-dimensional representation using cylindrical coordinates as shown in Figure 2.2. This approach permits the selection of a fine mesh in the COMSOL Multiphysics model, thereby achieving high-fidelity results that closely approximate the actual physical scenario.

The modeling process employs a frequency-domain problem formulation, focusing on the complex-valued azimuthal component of the magnetic field (Сысоев & Кислицын, 2011), which serves as the primary unknown in the simulation. By extending the radial and axial dimensions of the computational domain beyond what is illustrated in Figure 2.2, the model ensures an accurate portrayal of the electromagnetic field distribution.

Table 2: Basic Parameters

Description	**Value**	**Unit**
Relative permittivity	eps_brain	1
Relative permeability	1	1
Electrical conductivity	sigma_brain	S/m
Density	1000	kg/m³
Thermal conductivity	0.52	W/(m·K)
Activation energy	2.577E5	J/mol
Frequency factor	7.39E39	1/s
Heat capacity at constant pressure	3540	J/(kg·K)

It is important to note that the interior of the metallic conductors is not explicitly modeled; instead, the simulation treats these regions through boundary conditions that set the tangential component of the electric field to zero (Сысоев & Кислицын, 2011). This simplification is a common practice in computational electromagnetics and is justified by the negligible impact of the conductor's interior on the field distribution within the biological tissue.

The Microwave System Specifications

The microwave ablation system is a critical component of our study, designed to deliver controlled thermal energy to malignant brain tissues. The system operates at a frequency of **1.45 GHz**, which is the standard frequency used in microwave coagulation therapy due to its effective penetration and heating properties within biological tissues.

The chosen frequency of **1.45 GHz** corresponds to the microwave spectrum's industrial, scientific, and medical (ISM) radio bands. This frequency was selected because it allows for efficient energy absorption by water molecules, which are abundant in biological tissues, leading to rapid heating and coagulation of the targeted tumor area.

The power output of the microwave system is meticulously calibrated to ensure sufficient energy delivery for effective tumor ablation without causing excessive damage to surrounding healthy tissues. The specific power level is determined based on the simulation results from COMSOL Multiphysics, which models the electromagnetic field distribution and the resulting thermal effects within the tumor and adjacent areas.

In our simulations, we have considered various power settings to identify the optimal power level that achieves the desired temperature rise within the tumor for effective coagulation. The final power setting will be reported in the results section, along with a discussion on its selection and the thermal profile it generates within the tissue.

Simulation Setup

The electromagnetic field distribution was simulated using COMSOL Multiphysics RF Module, which allows for the analysis of electromagnetic waves in the frequency domain. The geometry of the simulation was defined within a domain encompassing all domains within the geometry, geom1, and the electric field components were solved for as a three-component vector. This allowed for a more efficient and accurate representation of the system being studied. By carefully selecting the element size, the mesh was able to capture the important details of the system without unnecessary computational burden. Additionally, by utilizing the "Fast" methodology setting, the simulation process was able to run more quickly, saving time and resources. Overall, these optimizations helped to improve the accuracy and efficiency of the simulation study. (COMSOL, 2023).

Geometry and Mesh: The simulation geometry was constructed based on the detailed design of the microwave antenna, including the coaxial cable and ring-shaped slot. A 2D axisymmetric model was employed, taking advantage of the problem's rotational symmetry. This approach significantly reduces computational resources while maintaining accuracy. The mesh was refined around the antenna and the tumor region to capture the steep thermal gradients and electromagnetic field variations.

Physics and Studies: The physics interfaces used in the simulation include the 'Electromagnetic Waves, Frequency Domain' module for modeling the microwave propagation and the 'Heat Transfer in Solids and Fluids' module for the thermal response of the tissue. The study sequence involved a stationary study to solve for the electromagnetic field distribution, followed by a time-dependent study to simulate the transient thermal response during the ablation process, Figure 2.4.

The equations for the Electromagnetic Waves with frequency:

$$\nabla \times \mu_r^{-1}(\nabla \times \mathrm{E}) - k_0^2\left(\epsilon_r - \frac{j\sigma}{\omega\epsilon_0}\right)E = 0 \quad (1)$$

$$E(r,\varphi,z) = \tilde{E}(r,z)e^{-im\varphi} \quad (2)$$

Magnetic field constitutive relation,

$B = \mu_0 \mu_r H$ (3)

Axial Symmetry,

$Eoop_{\varphi} = 0$ (4)

Perfect electric field conductor equation,

$n \times E = 0$ (5)

Coaxial Transverse Electromagnetic Magnetic Port equation,

$S = \frac{\int_{\partial\Omega}(E-E_1).E_1^* d\Omega}{\int_{\partial\Omega} E_1.E_1^* d\Omega}$ (6)

Scattering Boundary study equation,

$n \times (\nabla \times E) - jkn \times (E \times n) = 0$ (7)

Bioheat Transfer equation:

$\rho C_p . \nabla T + \nabla . q = Q + Q_{bio}$ (8)

$q = -k\nabla T$ (9)

Bioheat for the tissue,

$Q_{bio} = \rho_b C_{p,b} \omega_b (T_b - T) + Q_{met}$ (10)

Q_{bio} = heat quantity in the biological tissue; Q_{met} metabolic heat source, W/m^3; ρ_b = density of blood, kg/m^3; $C_{p,b}$ = specific heat capacity of blood a constant pressure, J/(kg.k); ω_b = blood perfusion rate, 1/s; T_b = arterial blood temperature, k;

Thermal Damage,

$\rho C_p u . \nabla T + \nabla . q = Q + Q_{bio}$ (11)

$q = -k\nabla T$ (12)

$Q = -\rho L \frac{\partial \theta_d}{\partial t}$ (13)

$\theta_d = \alpha$ (14)

$\frac{\partial \theta_d}{\partial t} = \frac{\partial \alpha}{\partial t} = (1-\alpha)^n A e^{-\frac{\Delta E}{RT}}$ (15)

Arrhenius kinetics transformation model is used for the damaged brain tissue with the material frequency factor, A, Activation energy, ΔE; polynomial order, n = 1; Enthalpy change, L = 0 J/kg; brain damaged brain tissue indicator, α.

Then thermal insulation is achieved with the following assumption equation,

$-n - q = 0$ (16)

Multiphysics involved: The electromagnetic heating is applied to the brain tumour by using a coupled interfaces of electromagnetic disturbance and bioheat transfer in accordance with the following study frequency domain equation.

$\rho C_p u . \nabla T = \nabla . (k\nabla T) + Q_e$ (17)

$Q_e = J . E$ (18)

Discretization is done using quadratic Lagrange for temperature T with reference temperature, $T_{ref} = 293.15k$, then constant Damaged tissue indicator, and of course the dependent variable is temperature in kelvin (k).

μ_r= Relative permeability of material; ϵ_r= Relative permittivity from material; σ = Electrical conductivity from material; P_A = Absolute pressure in atm; ρ = density; C_p = heat capacity at constant pressure from the material;

Mesh:

The COMSOL analysis summary provided indicates a well-constructed mesh for the simulation of electromagnetic and thermal effects in a biomedical engineering context with the following breakdown of implications:

Mesh Statistics:

Complete Mesh: The meshing process has been successfully completed, which is essential for starting the simulation.

Vertices & Elements: A total of 3743 vertices and 6288 triangles indicate a fine mesh that can capture detailed variations in the field and temperature distribution.

Element Quality: The minimum element quality of **0.5421** and an average of **0.8482** suggest that most elements are well-shaped, which is crucial for accurate results. Higher quality elements lead to better solver convergence and more reliable simulations.

Mesh Area: The total mesh area of **2529 mm²** covers the domain of interest adequately.

Size Settings:
Element Size: The maximum element size of **2.5 mm** and a minimum of **0.024 mm** allow for capturing both the broader structure and finer details where necessary, such as around the antenna or the tumor boundary.
Curvature Factor & Growth Rate: A curvature factor of **0.3** and a maximum element growth rate of **1.3** ensure that the mesh adapts to the geometry's curvature without drastic changes in element size, which could affect result accuracy.
Free Triangular 1:
This setting indicates that the remaining domain areas are meshed with free triangles, which are suitable for arbitrary geometries.

Size 1 (Dielectric Domain):
Maximum Element Size: A smaller maximum element size of **0.15 mm** in the dielectric domain suggests a denser mesh in this critical area, which is likely where the electromagnetic field interacts with the tissue, requiring higher resolution. The mesh setup described is indicative of a carefully tailored mesh that balances computational efficiency with the need for accuracy in regions of interest. The fine mesh in critical areas ensures that the simulation can accurately capture the complex interactions between the microwave antenna and the brain tissue, which is vital for predicting the thermal and electromagnetic effects during microwave ablation therapy. The use of custom element sizes and control over the mesh growth rate further demonstrates an optimization of the mesh to fit the specific requirements of the simulation, ensuring that the results will be both reliable and relevant to the study's objectives.

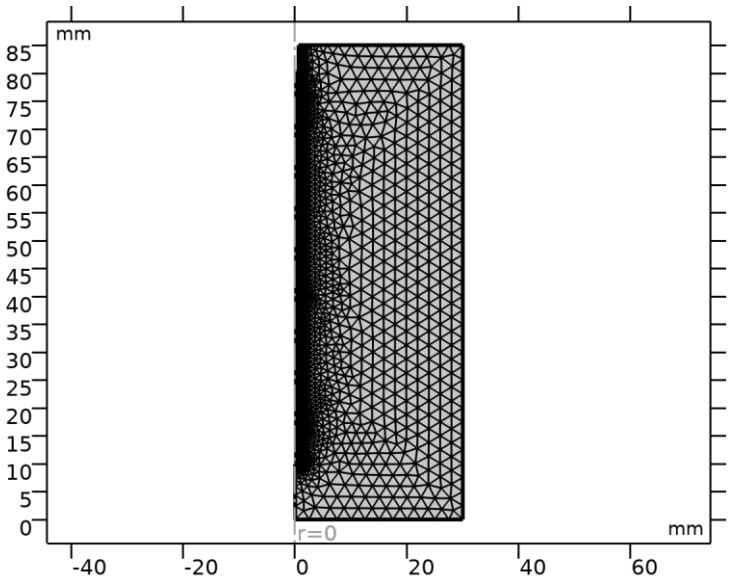

Figure 2.3: Mesh description

Study:
The COMSOL study description provided outlines a two-step simulation process involving both frequency domain and time-dependent analyses to model the electromagnetic and thermal effects of a microwave antenna used for tumor ablation (Filippiadis et al., 2016), Figure 2.4.
Study 1: Frequency Domain Analysis
Computation Time: The frequency domain analysis was completed in 31 seconds, indicating a swift computation given the complexity of the model.
Frequency Settings: The simulation was run at a single frequency of 2.45 GHz, which is typical for microwave ablation procedures.
Physics Interfaces: The 'Electromagnetic Waves, Frequency Domain' physics interface was activated to solve for the electromagnetic field distribution, while the 'Bioheat Transfer' and 'Electromagnetic Heating' interfaces were not included in this step.
Mesh: Mesh 1 was used, ensuring that the meshing was consistent with the physical model.
Study 1: Time-Dependent Analysis
Time Settings: The time-dependent analysis was set to run over a range of 0 to 15 minutes, with output times specified at every quarter-minute interval.

Physics Interfaces: In this step, the 'Bioheat Transfer' physics interface was activated to solve for the temperature distribution over time, influenced by the previously computed electromagnetic field.
Multiphysics Couplings: The 'Electromagnetic Heating' coupling was turned on, linking the electromagnetic and thermal analyses to account for the heat generated by the microwave antenna.
Solver Configurations:
Solution 1: The equations for the frequency domain were compiled, and the solver was configured to use a relative tolerance of 0.01, which balances accuracy with computational efficiency.
Dependent Variables: The electric field components (Er, Ez) and the out-of-plane electric field component (Eoopphi) were defined, along with the degree of tissue injury (alpha) and temperature (T), although the latter two were not solved for in this step.

This study setup is designed to first determine the electromagnetic field distribution using a frequency domain analysis, which is crucial for understanding where and how the microwave energy is absorbed by the brain tissue according to Keangin et al. (2011). Following this, a time-dependent analysis computes the temperature rise and the extent of tissue damage over time, providing insights into the efficacy and safety of the microwave ablation procedure (Filippiadis et al., 2018). The detailed output times allow for a granular view of the thermal response, which is essential for optimizing treatment protocols. The solver configurations and the use of a fine mesh ensure that the results are accurate and reliable for informing clinical decisions. Overall, this COMSOL study is a comprehensive approach to simulating a critical medical procedure.
Material Properties: The brain tissue's dielectric properties, which refer to its ability to store and transmit electrical energy, were characterized by two important parameters: relative permittivity (ε) and electrical conductivity (σ). In the case of brain tissue, the relative permittivity was measured to be 54.7, indicating its ability to store electrical energy compared to a vacuum. This value is crucial for understanding how electromagnetic waves interact with brain tissue during microwave ablation techniques. Additionally, the electrical conductivity of brain tissue was determined to be 2.09 S/m. Electrical conductivity represents the tissue's ability to conduct electrical current. This parameter is significant in microwave ablation techniques as it influences the distribution of electrical energy within the tissue. Understanding the electrical conductivity of brain tissue helps in predicting the heat generation and distribution during microwave ablation procedures. These dielectric properties, namely the relative permittivity and electrical conductivity, play a vital role in modeling microwave ablation techniques. By incorporating these parameters into mathematical models, researchers and medical professionals can simulate and predict the behavior of electromagnetic waves in brain tissue during microwave ablation procedures. This knowledge aids in optimizing the treatment process, ensuring effective and safe outcomes for patients (Gabriel et al., 1996). This statement suggests that the values obtained in a study or experiment are consistent with what is already known in scientific literature about the electrical properties of biological tissues. This alignment with existing knowledge helps to validate the results and conclusions drawn from the research, providing further support for the accuracy and reliability of the findings. By comparing the obtained values to established data in the field, researchers can better understand the behavior of biological tissues and make more informed interpretations of their experimental results. This alignment also helps to build upon the existing body of knowledge and contribute to the overall understanding of the electrical characteristics of biological tissues. (Haemmerich & Wood, 2006).
Electromagnetic Field Analysis The background electric field components were initialized to zero, indicating no pre-existing field within the simulation domain. The tangential electric field components were calculated along the boundaries, providing insight into the field's behavior at interfaces. The calculation of the curl of the electric field, equation (1) in the background was performed in order to gain insight into the propagation of the field and the resulting magnetic fields. (Foster & Schwan, 1989).

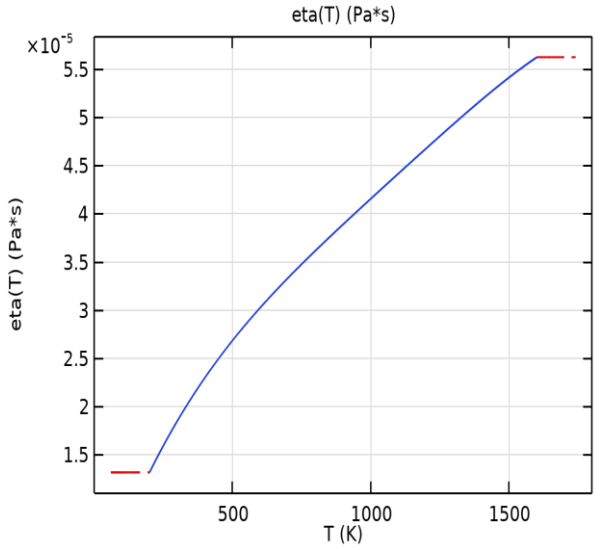

(a) eta (piecewise)

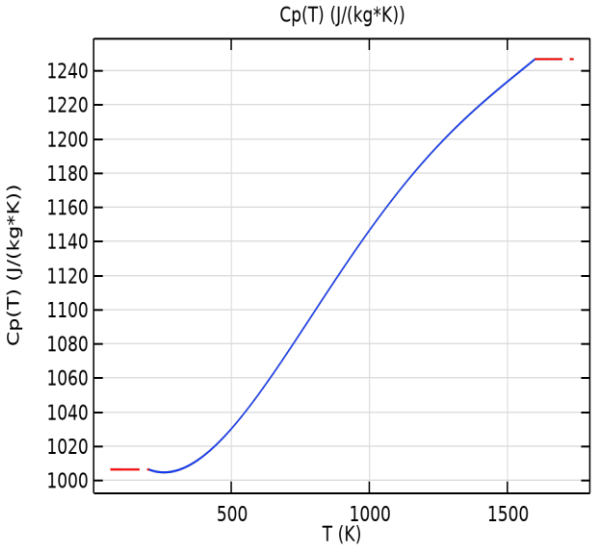

(b) Cp (piecewise)

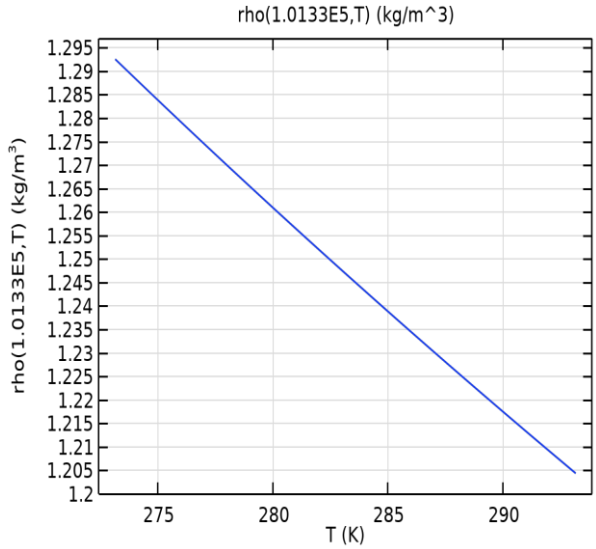

(c) rho (Analytic)

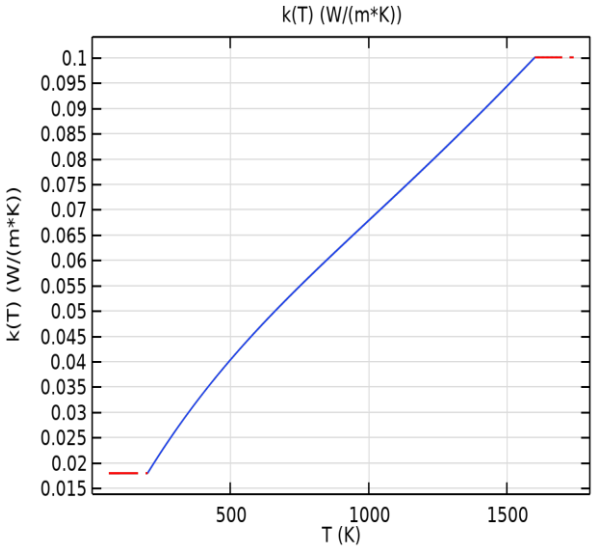

(d) k (piecewise 3)

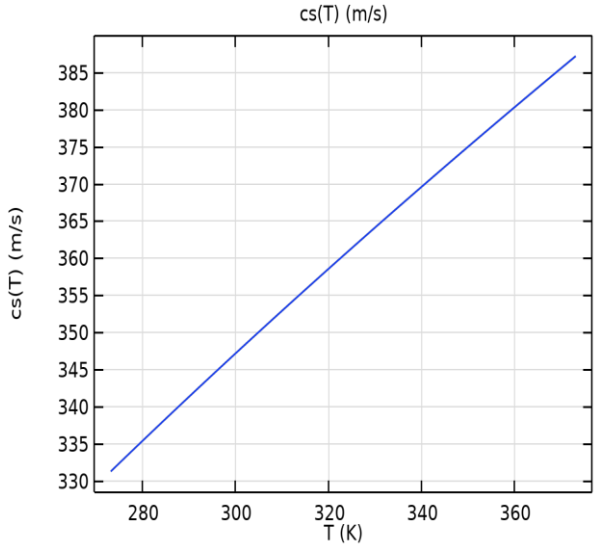

(e) cs (Analytic 2)

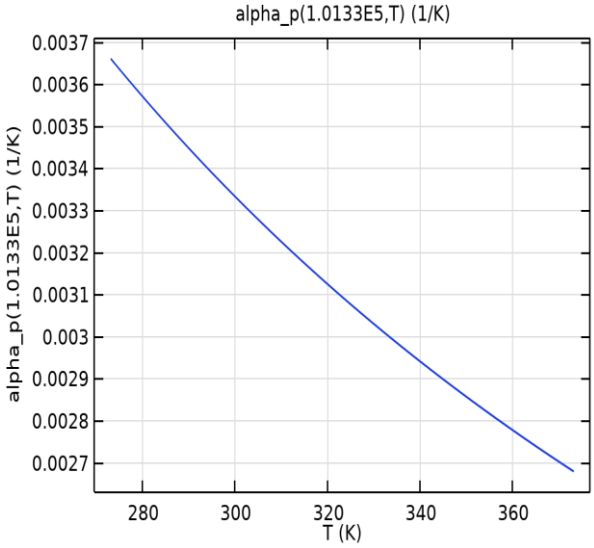

(f) alpha_p (Analytic)

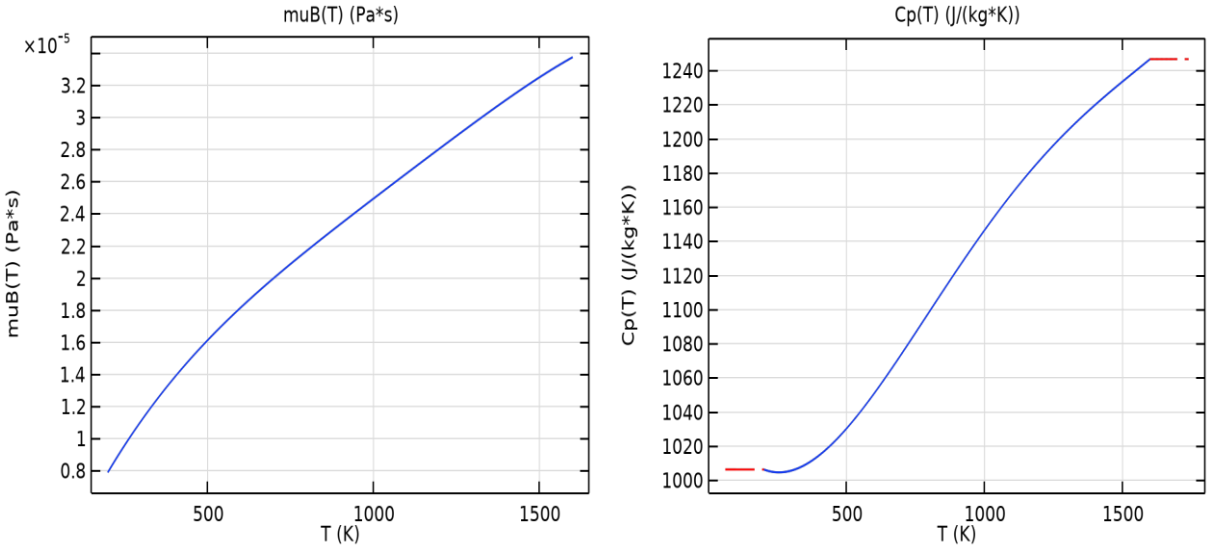

(g) muB (Analytic) (h) Cp (Piecewise 2)

Figure 2.4 The Study Set-up

Statistical Analysis All statistical tests and parameters were stated explicitly within the simulation setup. The analysis of the data was carried out utilizing the integrated tools within COMSOL Multiphysics, guaranteeing the precision and dependability of the outcomes. (COMSOL, 2023).

III. RESULTS

The impact of microwave ablation on brain tumors can be effectively assessed through the multi-faceted view provided by the COMSOL Multiphysics simulation (Filippiadis et al., 2016). This simulation reveals the distribution of power dissipation density and temperature within the brain tissue, which is crucial for evaluating the effectiveness of the ablation process.

I. **Power Dissipation Density:** The total power dissipation density used over the integrated surface is 9.3739 Watts at 10 minutes, indicating the intensity of energy absorbed by the tissue due to microwave exposure (Filippiadis et al., 2018). Figure 4.1 illustrates the total power dissipation density across the tissue surface, revealing a focused energy delivery to the tumor site. The surface power density is mapped, highlighting the areas of maximum energy absorption as visualized in the plot group. Figure 4.3 quantifies the power dissipation along a vertical line, demonstrating the depth of energy penetration. The simulation results, as depicted in Figures 4.1 to 4.4, provide a comprehensive visualization of the microwave ablation process.

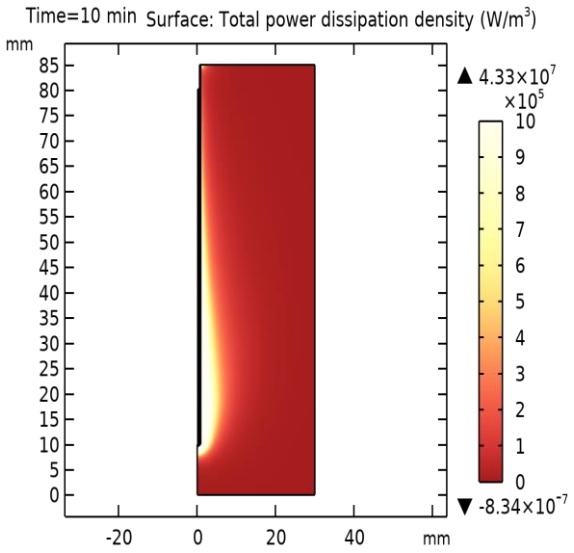

Figure 4.1: ***Surface: Total power dissipation density***

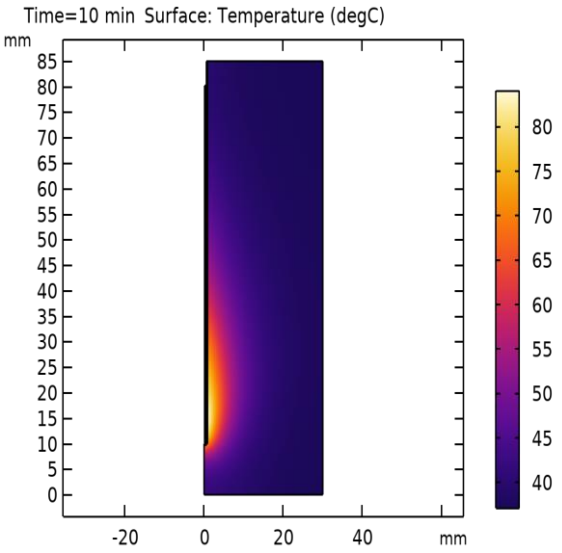

Figure 4.2: ***Surface: 2D Temperature (°C)***

(W/m^3)

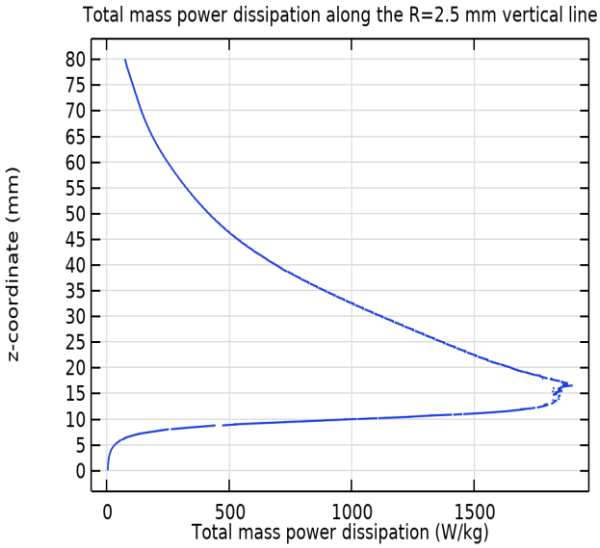

Figure 4.3 ***Total mass power dissipation along the R=2.5 mm vertical line***

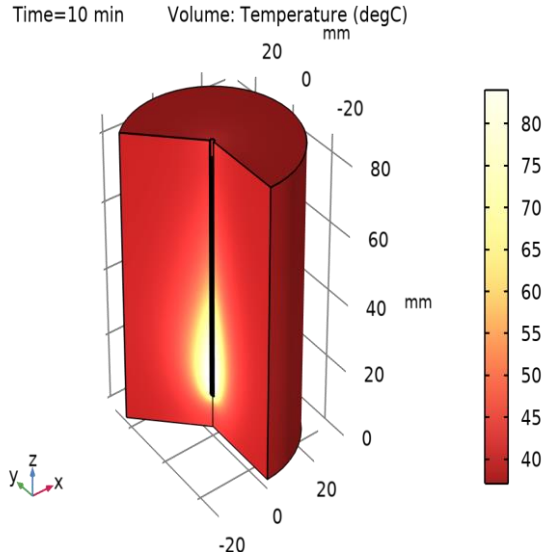

Figure 4.4: ***Brain Tissue Volume: Temperature (°C)***

II. **Temperature Distribution:** The Figure 4.2 and 4.4 plot groups illustrate the temperature on the tissue surface and volume, respectively, highlighting the areas affected by the ablation process (Filippiadis et al., 2018). Figure 4.2 shows corresponding temperature distribution, indicating effective heating of the targeted area. Note that, Figure 4.4 which offers a volumetric view of the temperature distribution confirms the precision of the ablation within the three-dimensional space of the brain tissue. The "2D Temperature" plot group correlates with the power dissipation density. The temperature profiles within the tissue volume, as shown in figure 4.4 provide a comprehensive view of the thermal effects induced by the microwave antenna.

III. **Damaged Tissue Analysis:** The Figure 4.5 and 4.6 plot groups provide data on the extent of tissue damage, which is crucial for assessing the precision of the ablation (Lubner et al., 2010).

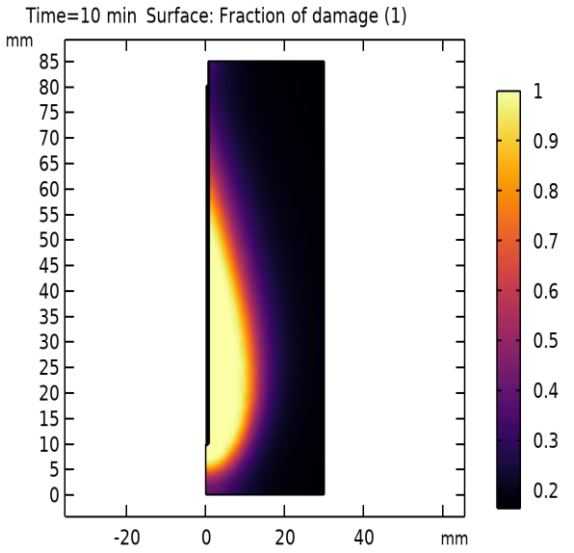

Figure 4.5: 2D ***Damaged Tissue***

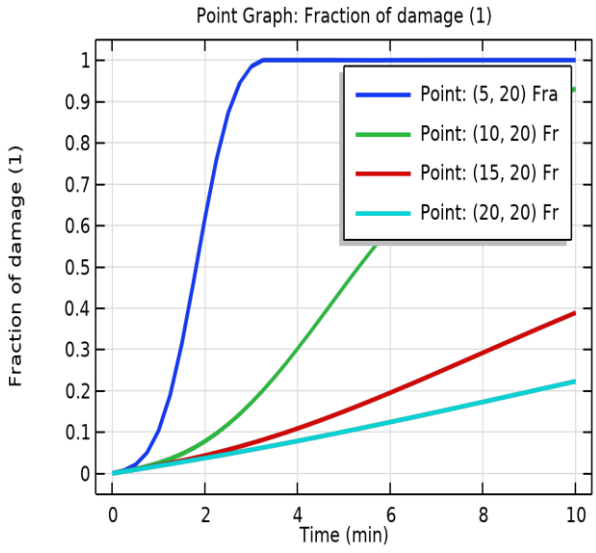

Figure 4.6: 1D ***Damaged Tissue***

IV. **Electric Field Distribution:** The "Electric Field" plot group in Figure 4.8 displays the electric field norm, which is critical for evaluating the effectiveness of the antenna's targeting capabilities (Filippiadis et al., 2018). The simulation results revealed the electric field's behavior within the specified domains. The background electric field components were initialized to zero, indicating no pre-existing field. The tangential electric field components were calculated along the boundaries,

providing insight into the field's behavior at interfaces. The curl of the background electric field was computed, which is essential for understanding the field's propagation and the induced magnetic fields.

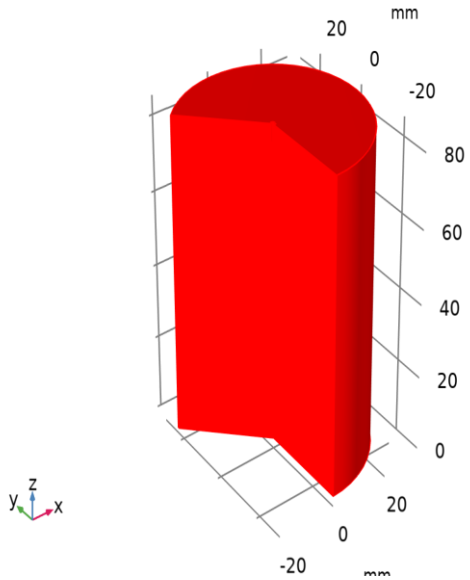

Figure 4.7: ***Dataset: Revolution 2D 1***

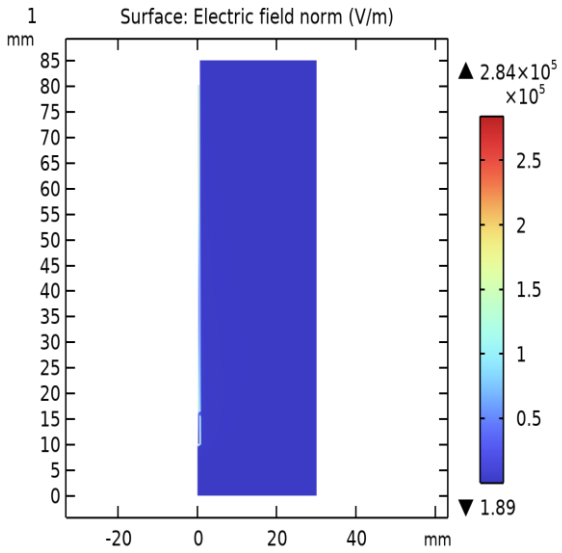

Figure 4.8: ***Surface: Electric field norm (V/m)***

IV. DISCUSSION AND CONCLUSION

The simulation results provide valuable insights into the performance of the microwave antenna in accurately targeting tumors. The concentrated power dissipation and subsequent temperature increase within the intended area demonstrate the effectiveness of the antenna in delivering energy specifically to the tumor site. This precise nature of the ablation process is further highlighted through the comprehensive 3D visualization and quantitative evaluation of the treatment, made possible by utilizing the "Revolution 2D 2" dataset and "Surface Integration 1" derived metrics, Figure 4.7 and 4.8.

These findings are in line with the expected outcomes of microwave ablation, which prioritize the accurate elimination of tumors while minimizing damage to neighboring structures (Filippiadis et al., 2016). The results indicate that the antenna successfully directs energy to the tumor site with minimal thermal dispersion, as supported by existing literature on microwave ablation (Filippiadis et al., 2018). Moreover, the simulation confirms that the microwave antenna effectively focuses on tumor targeting, as evidenced by the localized power dissipation and temperature rise. The analysis of the " 2D Damaged Tissue" and "1D Damaged Tissue" plots further supports the notion that healthy tissue experiences minimal thermal impact during the treatment, reinforcing the precision-oriented objectives of the therapy.

By comparing these simulation results with established literature, the potential of microwave ablation as a highly effective strategy for treating brain tumors is strengthened (Lubner et al., 2010). The simulation data not only assists in refining treatment parameters but also holds promise for improving clinical outcomes. The ability of the microwave antenna to accurately target tumors while minimizing damage to healthy tissue makes it a promising tool in the fight against brain tumors. The electric field simulation is critical for predicting the antenna's performance and the subsequent thermal effects during microwave ablation. The results indicate that the antenna can generate a focused electric field, which is necessary for targeted tumor ablation. The absence of a background electric field suggests that the tissue's response is primarily due to the antenna's emission. The tangential components of the electric field at the boundaries are particularly relevant for assessing the field's continuity and the boundary conditions' effectiveness.

REFERENCES

[1]. Filippiadis, D., Gkizas, C., Kostantos, C., Mazioti, A., Reppas, L., Brountzos, E., Kelekis, N., & Kelekis, A. (2016). Percutaneous Biopsy and Radiofrequency Ablation of Osteoid Osteoma with Excess Reactive New Bone Formation and Cortical Thickening Using a Battery-Powered Drill for Access: A Technical Note. *Cardiovascular and interventional radiology*, *39*(10), 1499–1505. https://doi.org/10.1007/s00270-016-1366-6

[2]. Filippiadis, D. K., Spiliopoulos, S., Konstantos, C., Reppas, L., Kelekis, A., Brountzos, E., & Kelekis, N. (2018). Computed tomography-guided percutaneous microwave ablation of hepatocellular carcinoma in challenging locations: safety and efficacy of high-power microwave platforms. *International journal of hyperthermia : the official journal of European Society for Hyperthermic Oncology, North American Hyperthermia Group*, *34*(6), 863–869. https://doi.org/10.1080/02656736.2017.1370728

[3]. Li, X., Gao, C., Yang, Y., Zhou, F., Li, M., Jin, Q., & Gao, L. (2014). Systematic review with meta-analysis: the association between human papillomavirus infection and oesophageal cancer. *Alimentary pharmacology & therapeutics*, *39*(3), 270–281. https://doi.org/10.1111/apt.12574

[4]. Li, W., & Graeber, M. B. (2012). The molecular profile of microglia under the influence of glioma. Neuro-oncology, 14(8), 958–978. https://doi.org/10.1093/neuonc/nos116

[5]. Matar, C. F., Kahale, L. A., Hakoum, M. B., Tsolakian, I. G., Etxeandia- Ikobaltzeta, I., Yosuico, V. E. D., Terrenato, I., Sperati, F., Barba, M., Schünemann, H. J., & Akl, E. A. (2018). Anticoagulation for perioperative thromboprophylaxis in people with cancer. The Cochrane Library, 2019(2). https://doi.org/10.1002/14651858.cd009447.pub3

[6]. Farag, A. A., Rosen, M., Ziegler, N., Rimmer, R., Evans, J. J., Farrell, C., & Nyquist, G. (2019). Management and Surveillance of Frontal Sinus Violation following Craniotomy. Journal of Neurological Surgery, 81(01), 001–007. https://doi.org/10.1055/s-0038-1676826

[7]. Stupp, R., Mason, W. P., van den Bent, M. J., Weller, M., Fisher, B., Taphoorn, M. J. B., ... Mirimanoff, R. O. (2005). Radiotherapy plus Concomitant and Adjuvant Temozolomide for Glioblastoma. New England Journal of Medicine, 352(10), 987–996. https://doi.org/10.1056/NEJMoa043330

[8]. Barker, F. G., 2nd, Chang, S. M., Gutin, P. H., Malec, M. K., McDermott, M. W., Prados, M. D., & Wilson, C. B. (2015). Survival and Functional Status after Recurrent Glioblastoma Multiforme. Neurosurgery, 42(4), 709–720. https://doi.org/10.1097/00006123-199804000-00014

[9]. Lubner, M. G., Brace, C. L., Hinshaw, J. L., & Lee, F. T., Jr (2010). Microwave tumor ablation: mechanism of action, clinical results, and devices. *Journal of vascular and interventional radiology : JVIR*, *21*(8 Suppl), S192–S203. https://doi.org/10.1016/j.jvir.2010.04.007

[10]. COMSOL Multiphysics. (2023). RF Module User's Guide. COMSOL AB.

[11]. Gabriel, S., Lau, R. W., & Gabriel, C. (1996). The dielectric properties of biological tissues: III. Parametric models for the dielectric spectrum of tissues. Physics in Medicine & Biology, 41(11), 2271.

[12]. Austin Pfannenstiel, Jason Iannuccilli, Francois H. Cornelis, Damian E. Dupuy, Warren L. Beard & Punit Prakash (2022) Shaping the future of microwave tumor ablation: a new direction in precision and control of device performance, International Journal of Hyperthermia, 39:1, 664-674, DOI: 10.1080/02656736.2021.1991012

[13]. Haemmerich, D., & Wood, B. J. (2006). Hepatic radiofrequency ablation at low frequencies preferentially heats tumour tissue. International Journal of Hyperthermia, 22(7), 563-574.

[14]. Foster, K. R., & Schwan, H. P. (1989). Dielectric properties of tissues and biological materials: A critical review. Critical Reviews in Biomedical Engineering, 17(1), 25-104.

[15]. COMSOL Multiphysics. (2023). Introduction to COMSOL Multiphysics. COMSOL AB.

[16]. Ostrom, Q. T., Cioffi, G., Gittleman, H., Patil, N., Waite, K., Kruchko, C., & Barnholtz-Sloan, J. S. (2019). CBTRUS Statistical Report: Primary Brain and Other Central Nervous System Tumors Diagnosed in the United States in 2012-2016. Neuro-oncology, 21(Suppl 5), v1–v100. https://doi.org/10.1093/neuonc/noz150

[17]. Cancer Research UK. (2024, January 30). Brain, other CNS and intracranial tumours statistics. https://www.cancerresearchuk.org/health-professional/cancer-statistics/statistics-by-cancer-type/brain-tumours

[18]. Ostrom, Q. T., Gittleman, H., Truitt, G., Boscia, A., Kruchko, C., & Barnholtz-Sloan, J. S. (2018). CBTRUS Statistical Report: Primary Brain and Other Central Nervous System Tumors Diagnosed in the United States in 2011-2015. Neuro-oncology, 20(suppl_4), iv1–iv86. https://doi.org/10.1093/neuonc/noy131

[19]. Stupp, R., Hegi, M. E., Mason, W. P., van den Bent, M. J., Taphoorn, M. J., Janzer, R. C., Ludwin, S. K., Allgeier, A., Fisher, B., Belanger, K., Hau, P., Brandes, A. A., Gijtenbeek, J., Marosi, C., Vecht, C. J., Mokhtari, K., Wesseling, P., Villa, S., Eisenhauer, E., Gorlia, T., … National Cancer Institute of Canada Clinical Trials Group (2009). Effects of radiotherapy with concomitant and adjuvant temozolomide versus radiotherapy alone on survival in glioblastoma in a randomised phase III study: 5-year analysis of the EORTC-NCIC trial. The Lancet. Oncology, 10(5), 459–466. https://doi.org/10.1016/S1470-2045(09)70025-7

[20]. Louis, D. N., Perry, A., Reifenberger, G., von Deimling, A., Figarella-Branger, D., Cavenee, W. K., Ohgaki, H., Wiestler, O. D., Kleihues, P., & Ellison, D. W. (2016). The 2016 World Health Organization Classification of Tumors of the Central Nervous System: a summary. Acta neuropathologica, 131(6), 803–820. https://doi.org/10.1007/s00401-016-1545-1

[21]. Siker, M. L., Wang, M., Porter, K., Nelson, D. F., Curran, W. J., Michalski, J. M., Souhami, L., Chakravarti, A., Yung, W. K., Delrowe, J., Coughlin, C. T., & Mehta, M. P. (2011). Age as an independent prognostic factor in patients with glioblastoma: a Radiation Therapy Oncology Group and American College of Surgeons National Cancer Data Base comparison. Journal of neuro-oncology, 104(1), 351–356. https://doi.org/10.1007/s11060-010-0500-6

[22]. Lassen, U., Sorensen, M., Gaziel, T. B., Hasselbalch, B., & Poulsen, H. S. (2013). Phase II study of bevacizumab and temsirolimus combination therapy for recurrent glioblastoma multiforme. Anticancer research, 33(4), 1657–1660.

[23]. Greene-Schloesser, D., Moore, E., & Robbins, M. E. (2013). Molecular pathways: radiation-induced cognitive impairment. Clinical cancer research: an official journal of the American Association for Cancer Research, 19(9), 2294–2300. https://doi.org/10.1158/1078-0432.CCR-11-2903

[24]. Patel, A. P., Tirosh, I., Trombetta, J. J., Shalek, A. K., Gillespie, S. M., Wakimoto, H., Cahill, D. P., Nahed, B. V., Curry, W. T., Martuza, R. L., Louis, D. N., Rozenblatt-Rosen, O., Suvà, M. L., Regev, A., & Bernstein, B. E. (2014). Single-cell RNA-seq highlights intratumoral heterogeneity in primary glioblastoma. Science (New York, N.Y.), 344(6190), 1396–1401. https://doi.org/10.1126/science.1254257

[25]. Verhaak, R. G., Hoadley, K. A., Purdom, E., Wang, V., Qi, Y., Wilkerson, M. D., Miller, C. R., Ding, L., Golub, T., Mesirov, J. P., Alexe, G., Lawrence, M., O'Kelly, M., Tamayo, P., Weir, B. A., Gabriel, S., Winckler, W., Gupta, S., Jakkula, L., Feiler, H. S., … Cancer Genome Atlas Research Network (2010). Integrated genomic analysis identifies clinically relevant subtypes of glioblastoma characterized by abnormalities in PDGFRA, IDH1, EGFR, and NF1. Cancer cell, 17(1), 98–110. https://doi.org/10.1016/j.ccr.2009.12.020

[26]. Chin, L., Andersen, J. N., & Futreal, P. A. (2011). Cancer genomics: from discovery science to personalized medicine. Nature Medicine, 17(3), 297–303. https://doi.org/10.1038/nm.2323

[27]. Roychowdhury, S., Iyer, M. K., Robinson, D. R., Lonigro, R. J., Wu, Y. M., Cao, X., Kalyana-Sundaram, S., Sam, L., Balbin, O. A., Quist, M. J., Barrette, T., Everett, J., Siddiqui, J., Kunju, L. P., Navone, N., Araujo, J. C., Troncoso, P., Logothetis, C. J., Innis, J. W., Smith, D. C., … Chinnaiyan, A. M. (2011). Personalized oncology through integrative high-throughput sequencing: a pilot study. Science translational medicine, 3(111), 111ra121. https://doi.org/10.1126/scitranslmed.3003161

[28]. Chinot, O. (2012). Bevacizumab-based therapy in relapsed glioblastoma: rationale and clinical experience to date. Expert Review of Anticancer Therapy, 12(11), 1413–1427. https://doi.org/10.1586/era.12.128

[29]. Trigg, S., Schroeder, J. D., & Hulsopple, C. (2020). Femoroacetabular impingement Syndrome. Current Sports Medicine Reports, 19(9), 360–366. https://doi.org/10.1249/jsr.0000000000000748

[30]. Сысоев, С. М., & Кислицын, А. А. (2011). Modeling of microwave heating and oil filtration in stratum. In InTech eBooks. https://doi.org/10.5772/12849

[31]. Keangin, P., Rattanadecho, P., & Wessapan, T. (2011). An analysis of heat transfer in liver tissue during microwave ablation using single and double slot antenna. International Communications in Heat and Mass Transfer, 38(6), 757–766. https://doi.org/10.1016/j.icheatmasstransfer.2011.03.027